

Comparative Theoretical Study of the Dissociation Process of the Isoelectronic Molecules BH_3CO , CH_2CO , HNCO , CO_2 and BH_3N_2 , CH_2N_2 , HN_3 , N_2O

Jacques Breulet* and Jacques Lievin

Laboratoire de Chimie Physique Moléculaire, Faculté des Sciences, CP. 160, Université Libre de Bruxelles, B-1050 Bruxelles, Belgium

An *ab initio* study of the electronic structure of several 22-electrons molecules is presented. The equilibrium geometries of their ground state are calculated at the SCF level using the 6-31G basis set and are found to be in good agreement with the experimental geometries. The dissociation process of these molecules leading to the isoelectronic products CO or N_2 on the one hand and BH_3 , CH_2 , NH and O on the other hand is studied. The least-energy dissociation paths of the ground states determined at the SCF level are compared on the basis of electron density interactions. The dissociation energies corresponding to the two lowest dissociation channels are calculated. In these calculations, the correlation energy is taken into account using a non-variational method developed previously. The calculated values of dissociation energies are in good agreement with the existing experimental values. The results permit to predict values for HNCO , BH_3CO and CH_2N_2 and to confirm the instability of BH_3N_2 .

Key words: Boron carbonyl – Carbon dioxide – Diazaborane – Diazomethane – Ethenone – Hydrazoic acid – Isocyanic acid – Nitrogen oxide (N_2O) – Dissociation of ~.

1. Introduction

In two preceding papers, the electronic structure of the isoelectronic molecules diazomethane (CH_2N_2) [1] and hydrazoic acid (HN_3) [2] has been studied

* Aspirant du Fonds National Belge de la Recherche Scientifique.

theoretically by means of LCAO-MO-SCF calculations. The comparison of the two systems and particularly of their respective dissociation pathway has helped to understand their electronic structure. It seemed interesting to us to pursue this work with a comparative study of the electronic structure of all other isoelectronic molecules composed of CO or N₂ on the one hand and one of the radicals BH₃, CH₂, NH or O on the other hand. These molecules are boron carbonyl (BH₃CO), ethenone (CH₂CO), isocyanic acid (HN₃), carbon dioxide (CO₂) – referred below as the “CO-molecules” – and diazoborane (BH₃N₂), diazomethane (CH₂N₂), hydrazoic acid (HN₃) and nitrogen oxyde (N₂O) – referred below as the “N₂-molecules”.

The calculations concern the equilibrium geometries, the least energy dissociation pathways and the dissociation energies. For this last point, we have used an economical method for the calculation of the correlation energy. This method is based on the separation of the correlation energy into internal and non-internal contributions [3].

The electronic states and configurations and the corresponding symmetry groups at equilibrium geometries are given in Table 1 for the molecules cited above and in Table 2 for their dissociation products. The ground state of all these 22-electrons molecules is a singlet and gives rise, by Wigner–Witmer dissociation,

Table 1. Isoelectronic molecules

Mol.	Sym. group	State	Configuration
CO ₂	<i>D</i> _{∞h}	¹ Σ _g ⁺	1σ _u ² (1-3)σ _g ² 2σ _u ² 4σ _g ² 3σ _u ² 1π _u ⁴ 1π _g ⁴
N ₂ O	<i>C</i> _{∞v}	¹ Σ _g ⁺	(1-6)σ ² 1π ⁴ 7σ ² 2π ⁴
HN ₃	<i>C</i> _s	¹ A'	(1-6)a' ² 1a'' ² (7-9)a' ² 2a'' ²
HNCO	<i>C</i> _s	¹ A'	ditto
CH ₂ N ₂	<i>C</i> _{2v}	¹ A ₁	(1-6)a ₁ ² 1b ₂ ² 1b ₁ ² 7a ₁ ² 2b ₂ ² 2b ₁ ²
CH ₂ CO	<i>C</i> _{2v}	¹ A ₁	(1-7)a ₁ ² 1b ₂ ² 1b ₁ ² 2b ₂ ² 2b ₁ ²
BH ₃ N ₂	<i>C</i> _{3v}	¹ A ₁	(1-6)a ₁ ² 1e ⁴ 7a ₁ ² 2e ⁴
BH ₃ CO	<i>C</i> _{3v}	¹ A ₁	ditto

Table 2. Dissociation products

Mol.	Sym. group	State	Configuration
N ₂	<i>D</i> _{∞h}	¹ Σ _g ⁺	1σ _g ² 1σ _u ² 2σ _g ² 2σ _u ² 1π ⁴ 3σ _g ²
CO	<i>C</i> _{∞v}	¹ Σ _g ⁺	(1-4)σ ² 1π ⁴ 5σ ²
O	<i>K</i> _h	³ P	1s ² 2s ² 2p ⁴
		¹ D	
NH	<i>C</i> _v	³ Σ _g ⁻	1σ ² 2σ ² 3σ ² 1π ²
		¹ Δ	
CH ₂	<i>C</i> _{2v}	³ B ₁	1a ₁ ² 2a ₁ ² 1b ₂ ² 3a ₁ 1b ₁
		¹ A ₁	1a ₁ ² 2a ₁ ² 1b ₂ ² 3a ₁ ²
BH ₃	<i>D</i> _{3h}	¹ A ₁	1a ₁ ² 2a ₁ ² 1e ⁴

to N_2 or CO in their ground state ($^1\Sigma_g^+$, $^1\Sigma^+$ respectively) and to the first excited singlet state of $O(^1D)$, $NH(^1\Delta)$ and $CH_2(^1A_1)$.

2. Methods of Calculation

2.1. SCF Calculations

The SCF energies, used for the derivation of the equilibrium geometries as described in sections 3 and 4, the atomic integrals used in the CI calculations (cf. 2.2.1), the Mulliken population analyses (cf. 2.2.2) have been calculated with the program GAUSSIAN 76 [4] for closed shell structures. The method of Davidson (OCBSE) [5] coded by Morokuma and Iwata [6] has been used for open-shell RHF calculations. The calculations involve three gaussian basis sets:

- the minimal basis set STO-3G [7]
- the “double-zeta quality” basis set 6-31G [8]
- the polarized basis set 6-31G** [9]

2.2. Correlation Energy Calculations. Dissociation Energies

Although the SCF model, when used with appropriate basis sets, can provide us with interesting informations about chemical properties of the molecules (geometries, for example), the energetical results are often disappointing. In the case of bond dissociation energies, for example, even very elaborate basis sets approaching the Hartree–Fock limit can lead to chemically meaningless results. The difference between the Hartree–Fock energy and the exact non-relativistic solution, the so-called “correlation energy” is essential in this kind of calculations. The application of purely variational methods (CI/MCSCF) to the molecules of interest to this work should be very expensive and even impossible. That is why we have used a simplified method, that has been successfully applied to the calculation of the dissociation energy of several di- and polyatomic molecules [3]. It is inspired from the partitioning of Sinanoğlu and Oksüz [10] who recognize three contributions to the correlation energy: internal, semi-internal and all-external. These three contributions are characterized by different types of electron pair excitations with respect to a particular subspace defined in the complete orbital space. This subspace, called the “Hartree–Fock sea” is composed of the shells partially or completely occupied in the Hartree–Fock Slater determinant, i.e. the $1s$, $2s$ and $2p$ orbitals for first row atoms. The three possible types of pair excitations are the following:

- excitations from filled to vacant orbitals within the H.F. sea giving rise to internal correlation
- excitations where one electron shifts within the H.F. sea and the other outside, giving rise to semi-internal correlation
- biexcitations from the inside to the outside of the H.F. sea, giving rise to all-external correlation

In our method, we propose to separate the internal and non-internal (= semi-internal + all-external) correlation energy contributions

$$E_{\text{CORR}}^{\text{TOT}} \approx E_{\text{CORR}}^{\text{I}} + E_{\text{CORR}}^{\text{NI}}.$$

2.2.1. Internal correlation energy

We postulate that it is possible to calculate the internal correlation energy by means of a configuration interaction calculation in a minimal basis set of all the biexcitations with respect to the reference determinant. The minimal basis set is particularly advantageous because all the molecular orbitals correlate asymptotically to the valence orbitals of the constituent atoms. This implies that the molecular orbital in a minimal basis set, occupied as well as virtual, belong to a “molecular H.F. sea” so that all the biexcitations give rise to internal correlation energy. This fact allows us to avoid a difficult optimization of a valence orbital subspace as it is necessary with an extended basis set.

Several tests have been made on a few small systems comparing the internal correlation energy calculated by a minimal basis set CI on the one hand with an iterative MCSCF/CI procedure using an extended basis set on the other hand [3]. The comparison supports the assumption of the validity of the use of a minimal STO-3G CI.

The CI calculations were run with the programs written by Whitten and his collaborators [11] adapted to GAUSSIAN 76.

2.2.2. Non-internal correlation energy

This part is evaluated by an “atoms-in-molecule” method. The basic idea consists of evaluating a sum of average non-internal correlation energy of atomic configurations of the constituent atoms of the molecule. These non-internal energies are known [12, 13]. Each of these atomic contributions is weighted by the electronic occupation of the configuration. This occupation probability is calculated on the basis of a Mulliken population analysis [14]. Indeed, the substitution of the notion of occupation probability to the initial notion of population breakdown allows us to define a simultaneous occupation probability of several atomic spinorbitals by simple product of the individual probabilities. For a given molecule we can thus associate to each atomic configuration of the constituent atoms an occupation probability.

For each atom X_i of the given molecule, we have then $K(X_i)$ atomic configurations $\tilde{S}_k(\tilde{S}_k(X_i); k = 1, K(X_i))$ with the associated occupation probability $\tilde{P}_k(X_i)$. Having determined the average non-internal correlation energy $E_{\text{CORR}}^{\text{AT}}(\tilde{S}_k(X_i))$ one can then calculate the molecular non-internal correlation energy:

$$E_{\text{CORR}}^{\text{NI}}(X_1 \cdots X_N) = \sum_{i=1}^N \sum_{k=1}^{K(X_i)} \tilde{P}_k(X_i) E_{\text{CORR}}^{\text{AT}}(\tilde{S}_k(X_i)).$$

This formalism, which has been described in detail elsewhere [3] implies that the molecular orbitals have to be expressed unambiguously in terms of purely atomic basis orbitals; this is achieved with a minimal basis set like STO-3G.

2.2.3. Dissociation energies

The dissociation energies were calculated using two basis sets: the minimal STO-3G basis set to derive the two parts of the correlation energies and the extended 6-31G** basis set for the SCF energies. It has been shown previously [3] that the 6-31G equilibrium geometries were convenient to perform these separate calculations.

2.3. Electronic Distribution Plots

An illustration of the electronic distribution in a molecule can be very helpful in the study of the molecular size, orbital shapes and electronic rearrangements during bond formation. In our study it illustrates the interpretation of the electronic structures and the dissociation mechanism. The program MOPLOT [15] calculates the charge density at each point of a given plane of the molecule. In order to facilitate the interpretation this particular plane can be displayed as a surface plot. An adaptation of the program HIDE [16] provides us with three dimensional representation of this surface plot on a digital CALCOMP tracer. The basis set used here was again the STO-3G basis set owing to the quality of its density representation with respect to its very low cost.

3. Equilibrium Geometries. Electronic Structure

In Fig. 1 we define the standard nomenclature used here for the geometrical parameters of all the molecules. The equilibrium geometries have been obtained by fitting the energy values to coupled quadratic equations involving all the parameters. Coupling terms include all possibilities between adjacent in plane parameters (e.g. $R_1\beta$, R_1R_2 , $R_2\beta$, $\alpha\beta$, ...).

The torsion of the molecules has not been considered here because the influence of this parameter on the energy has been found to be negligible in the cases of CH_2N_2 [1] and HN_3 [2].

It is now established that the basis 6-31G is particularly well-adapted for the calculation of the geometrical parameters at the SCF level in view of its good

Fig. 1. Geometrical parameters. The heavy atoms L_1 and L_2 represent either N_2 or CO , the heavy atom L_3 symbolizes O, N, C or B. The angle γ_0 determines the angle between the bond C—H and the bisector of CH_2 or the angle between the bond B—H and the axis of order three in BH_3 . γ_0 is identically zero in NH and absent in O

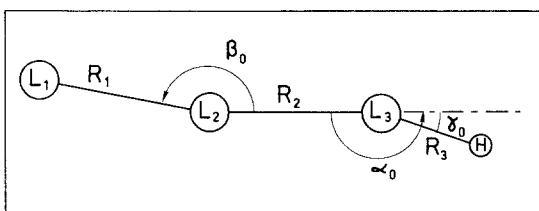


Table 3. Equilibrium geometries of the CO-molecules. Units are angströms and degrees

Mol.		R_1	R_2	R_3	Param.			$R_1 + R_2$
					α_0	β_0	γ_0	
CO ₂	exp [17]	1.160	1.160	—	—	180	—	2.320
	calc. 1 ^a	1.173	1.173	—	—	180	—	2.346
	calc. 2 [18]	1.159	1.159	—	—	180	—	2.318
HNCO	exp [19]	1.166	1.214	0.995	124	173	0	2.380
	calc. 1 ^a	1.191	1.186	0.990	150	175	0	2.377
	calc. 2 [20]	1.151	1.199	0.994	125	175	0	2.350
CH ₂ CO	exp [21]	1.161	1.316	1.078	180	180	61	2.477
	calc. 1 ^a	1.178	1.310	1.079	180	180	60	2.488
	calc. 2 [22]	1.17	1.31	1.07	180	180	61	2.48
BH ₃ CO	exp [23]	1.14	1.53	1.25	180	180	77	2.67
	calc. 1 ^a	1.136	1.611	1.209	180	180	76	2.747

^a this work**Table 4.** Equilibrium geometries of the N₂-molecules

Mol.		R_1	R_2	R_3	Param.			$R_1 + R_2$
					α_0	β_0	γ_0	
N ₂ O	exp. [24]	1.128	1.184	—	—	180	—	2.312
	calc. 1 ^a	1.112	1.242	—	—	180	—	2.354
	calc. 2 [25]	1.147	1.240	—	—	180	—	2.387
HN ₃	exp. [26]	1.134	1.243	1.015	108.8	171.3	0	2.377
	calc. 1 ^a	1.125	1.272	1.021	111	170	0	2.397
	calc. 2 [27]	—	—	—	112	172	0	—
CH ₂ N ₂	exp. [28]	1.139	1.300	1.075	180	180	63	2.439
	calc. 1 ^b	1.148	1.289	1.08	180	180	61.5	2.437
	calc. 2 [29]	1.189	1.282	1.078	180	180	60.8	2.471

^a this work^b basis set (10s5p; 4s) of Whitten [30] contracted to (4s2p; 2s)

quality to price ratio. That is why we have systematically used it for our geometry calculations.

Calculated and experimental results are listed in Tables 3 and 4 for the molecules containing CO and N₂ respectively. The values calculated in this work (calc. 1) are also compared to other theoretical values of at least the same level of accuracy (calc. 2). For BH₃N₂ no stable equilibrium geometry has been found.

The results show the generally good quality of the 6-31G basis set. The bond lengths are in agreement with the experimental data within 0.02 Å in almost all cases except for the very bad results obtained for B—H and B—C. This could be attributed to a poor optimization of the basis set for atom B, as can be

suggested by the case dependent discrepancy observed between calculated and experimental equilibrium distances for the ground states of the B_2 , BO and BF molecules: 1.78 Å (calculated) compared to 1.59 Å (experimentally) for B_2 , 1.21 Å to 1.204 Å for BO and 1.32 Å to 1.26 Å for BF. It may also be noted that bond lengths of N—N(L_2-L_3) in N_2O and HN_3 are slightly overestimated; the sum (R_1+R_2) is in most cases in better agreement with the corresponding experimental values than the individual R_1 and R_2 values. This feature was already pointed out in the previous works [1, 2].

The angles are also well reproduced except α_0 in HNCO for which our calculated value (150°) is qualitatively false. This strong disagreement prompted us to optimize this parameter separately using the 6-31G** basis set, keeping the other parameters frozen at their 6-31G equilibrium values. This leads to $\alpha_0 = 130^\circ$ which is in much better agreement with experiment (124°). This important basis effect, which is confirmed by the calculation of McLean et al. (125°) [20], seems to be limited to HNCO only. Indeed, the calculated α_0 value of HN_3 , an entirely similar molecule, is very good. In this context, it may be noted that the non linearity of HN_3 was previously verified by CI calculations and also by incorporating a β^3 term in the polynomial expression of the energy [3]. Similar calculations were not carried out here for HNCO on account of other theoretical verifications of that phenomenon [20].

In Fig. 2 we have plotted the electronic densities of the different molecules at equilibrium geometry in a given molecular plane. This plane is arbitrary in the

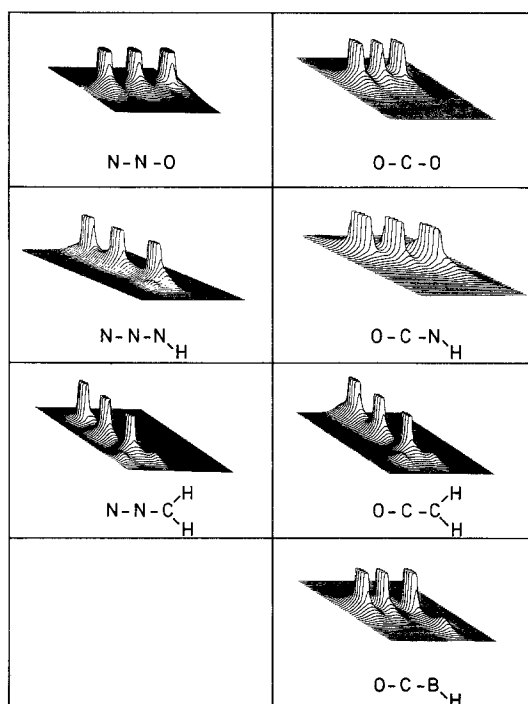


Fig. 2. Electronic densities calculated in a selected molecular plane (see text) at equilibrium geometries (STO-3G basis set)

point groups $C_{\infty v}$ and $D_{\infty h}$, corresponds to the molecular plane in C_s and C_{2v} , and contains CO and one of the B—H bonds in BH_3CO . The comparison of the electronic distributions shows that in all cases the bonds CO have a larger electronic density than the corresponding N—N bonds in “sister” molecules. Also the lone pairs of the N atoms are apparent. These two points will be helpful in the discussion of the dissociation mechanisms (section 4). In BH_3CO the weakness of the bond B—C is revealed by the quasi absence of electronic density.

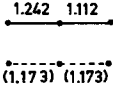
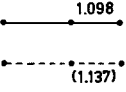
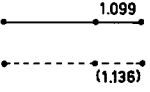
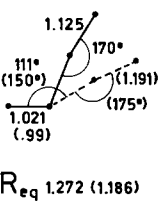
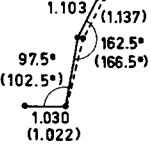
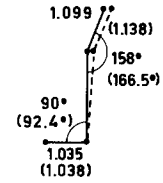
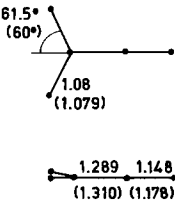
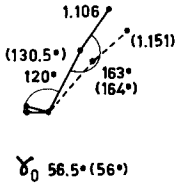
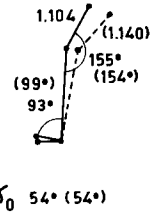
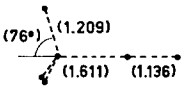
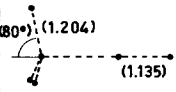
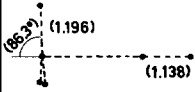
Mol.	R_{eq}	$R = 3.0 \text{ a.u.}$	$R = 4.0 \text{ a.u.}$
N_2O CO_2			
NH_3 HNCO			
CH_2N_2 CH_2CO			
BH_3CO			

Fig. 3. Comparison of the least energy dissociation paths (6-31G basis set). Full lines refer to N_2 -molecules, dotted lines to CO-molecules. Values of the geometrical parameters are in parentheses for the CO-molecules. Bond lengths in Å

4. Least-energy Dissociation Paths

Simultaneous minimization of the ground state energy as a function of all parameters reported in Fig. 1 was carried out at two selected values of the dissociation coordinate $R_{L_2L_3}$ (3.0 and 4.0 a.u.) in addition to the equilibrium distance. As described in section 3 optimized geometries were derived from a quadratic expression of the potential including coupling between interacting parameters. Fig. 3 presents a comparison of the least-energy dissociation paths of all the systems. It appears at first sight that the CO and N₂ molecules behave qualitatively in a similar way.

On the other hand, the BH₃- and O-molecules dissociate linearly while the CH₂- and NH-molecules exhibit a non-linear behaviour. The comparison between CH₂N₂ and HN₃ has been discussed previously [2] on the basis of the interaction between the Π structure on the N₂ molecule, the L₃H bond densities and the L₃ lone pair.

At large $R_{L_2L_3}$ distance, the equilibrium angle between the two molecules is the same ($\sim 90^\circ$) for the CH₂- and NH-molecules, corresponding to the direction of lowest repulsion of the L₁L₂ Π structure directed between the L₃H bond(s) and the L₃ lone pair(s).

Oppositely, at short range the geometrical behaviour of the CH₂- and NH-molecules is different:

(1) in the case of CH₂, the existence of the two CH bond densities on both sides of the L₁L₂L₃ plane prevents the formation of the L₁L₂L₃ Π -structure perpendicular to this plane. This feature explains the symmetry change ($C_s \rightarrow C_{2v}$) which takes place, resulting in a planar molecule at equilibrium geometry. This structure has furthermore a linear L₁L₂L₃ skeleton as a consequence of the symmetric interaction between the two CH bonds and the Π -density.

(2) in the case of NH, the presence of a single NH bond does not impose a change of symmetry plane (conservation of C_s symmetry) to allow the formation of the perpendicular L₁L₂L₃ Π -structure. However, the L₁L₂L₃ Π -structure remains non-linear as a result of its asymmetric repulsion with the NH bond density on the one hand and the N lone pair on the other hand.

To illustrate this last case, Fig. 4 shows the evolution of the electronic density of HN₃ along its dissociation path. On this figure, we note:

(1) the progressive decrease of the L₂L₃ density

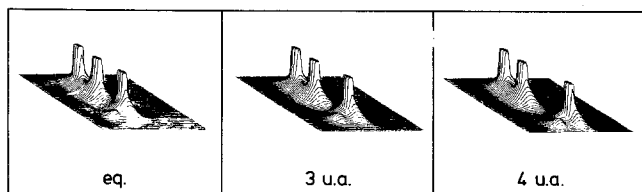


Fig. 4. Evolution of the electronic density of HN₃ along the least-energy dissociation path. (STO-3G basis set)

(2) the relative positions of the NH bond density and the N lone pair which lead to the non-linear structure.

The above discussion can be extended to justify the linear dissociation behaviour of the BH₃- and O-molecules. The BH₃-group imposes a triple symmetric interaction between the BH bonds and the L₁L₂ Π-structure which leads to a linear L₁L₂L₃ structure at every distance. In the case of N₂O and CO₂ the spherical symmetry of the oxygen atom does not impose any particular angular repulsions on its partner (N₂ or CO) and it is therefore the linear L₁L₂L₃ structure which gives the strongest binding, since it preserves the Π-structure even at larger distances.

Some other relevant features appearing on Fig. 3, can be pointed out:

(1) The transformation from planar BH₃ (*D*_{3h}) at infinite separation to pyramidal BH₃ (*C*_{3v}) at shorter range can be explained by the progressive repulsion between the BH bond densities and the L₁L₂ Π-structure

(2) the larger L₂L₃H angles for the non-linear CO-molecules as compared to the corresponding N₂-molecules can be attributed to the CO molecule Π density which is larger than the N₂ one.

5. Dissociation energies

It is difficult to find accurate experimental data for dissociation energies of molecules such as those studied here. Thermochemical data that allow to calculate unambiguously this property were found only for N₂O, CO₂ and CH₂CO. For the other molecules, photochemical data were available, but owing to difficulties in interpretation, the measurement leads sometimes only to upper (or lower) limits of the dissociation energy.

The calculated values for *D_e* are compared to the experimental ones in Tables 5 and 6 for the N₂- and CO-molecules respectively. For the molecules with CH₂, NH or O, the two first dissociation channels are taken into account; one is spin-forbidden and leads to the fragment in its fundamental triplet state, the

Table 5. Dissociation energies (eV) of N₂-molecules

Process (X = N ₂ (¹ Σ _g ⁺))	<i>D_e</i> (calc)	<i>D_e</i> (exp)
N ₂ O(¹ Σ ⁺) → X + O(³ P)	1.06	1.82 [31]
→ X + O(¹ D)	3.30	3.79 ^a [31]
HN ₃ (¹ A') → X + NH(³ Σ ⁻)	0.44	1.0 [33]
→ X + NH(¹ Δ)	2.29	2.57 [33]
CH ₂ N ₂ (¹ A ₁) → X + CH ₂ (³ B ₁)	0.87	2.03 [34]/2.12 [35]
→ X + CH ₂ (¹ A ₁)	1.87	1.6–1.78 [36, 37]
BH ₃ N ₂ (¹ A ₁) → X + BH ₃ (¹ A' ₁)	0	—

^a based on a term energy of O(¹D) of 1.97 eV [32]

Table 6. Dissociation energies (eV) of CO-molecules

Process ($X = \text{CO}(^1\Sigma^+)$)	D_e (calc)	D_e (exp)
$\text{CO}_2(^1\Sigma_g^+) \rightarrow X + \text{O}(^3P)$	5.68	5.63 [31]
$\rightarrow X + \text{O}(^1D)$	7.91	7.54 ^a [31]
$\text{HNCO}(^1A') \rightarrow X + \text{NH}(^3\Sigma^-)$	4.39	—
$\rightarrow X + \text{NH}(^1\Delta)$	6.25	—
$\text{CH}_2\text{CO}(^1A_1) \rightarrow X + \text{CH}_2(^3B_1)$	3.44	3.6 [38, 39]
$\rightarrow X + \text{CH}_2(^1A_1)$	4.44	4.0 ^b [38, 39]
$\text{BH}_3\text{CO}(^1A_1) \rightarrow X + \text{BH}_3(^1A'_1)$	0.78	—

^a same as Table 5^b based on a term energy of $\text{CH}_2(^1A_1)$ of 0.4 eV [40]

other is Wigner–Witmer allowed and gives the fragment in its first singlet excited state.

The agreement found between the values calculated here and the thermochemical data for CO_2 , CH_2CO and N_2O , in accordance with previous tests on smaller

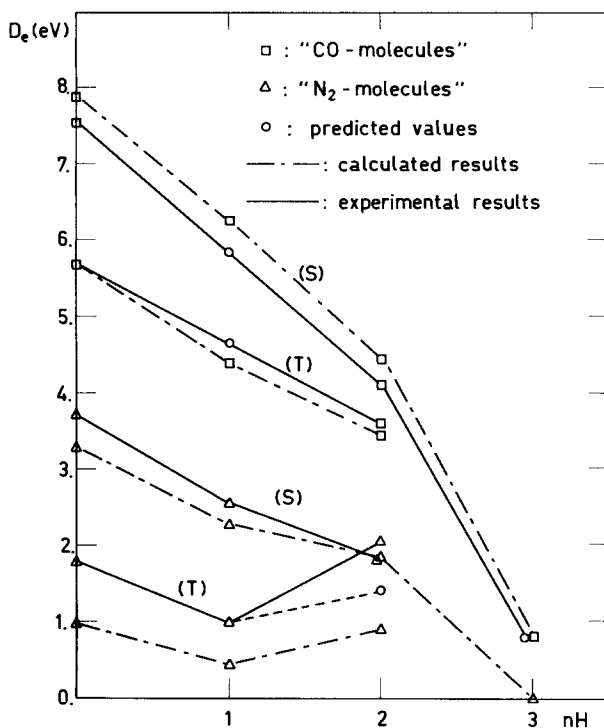


Fig. 5. Calculated and experimental dissociation energy values as a function of the number of hydrogen atoms in the molecules. (S) refers to the Wigner–Witmer path, (T) to the spin-forbidden one

systems [3] allows us to consider the whole set of calculated values as good approximations to the true values. This conclusion is reinforced by the data shown in Fig. 5 where we have plotted the diagrams of the dissociation values (calculated and experimental) with respect to the number of hydrogen atoms in the molecules, (*S*) refers to the Wigner–Witmer path and (*T*) to the spin-forbidden one. One can observe the quasi-parallelism between the calculated and experimental plots. The data in Tables 5 and 6 and in Fig. 5 allow us to make theoretical predictions:

- (1) In the case of HNC₂O, on account of the calculated points, we predict 5.8 eV and 4.65 eV as approximations for the actual values of dissociation energy for the Wigner–Witmer and spin forbidden dissociation respectively.
- (2) The experimental dissociation energy value for the dissociation of CH₂N₂ into N₂(¹Σ_g⁺) and CH₂(³B₁) – curve “*T*” – that was at our disposal is ~2.0 eV [34; 35].

This was not obtained by direct observation of CH₂(³B₁) but on account of $\Delta H_f^0(\text{CH}_2\text{N}_2) > 51$ kcal/mol obtained by these authors and $\Delta H_f^0(\text{CH}_2) = 93$ kcal/mol. The former value seems to be questionable. On the contrary, several authors have obtained values for the Wigner–Witmer dissociation (CH₂N₂ to CH₂(¹A₁) and N₂(¹Σ_g⁺)) from 1.6 eV to 1.8 eV. Among them, a value of 1.6 eV was obtained by direct observation of CH₂(¹A₁) during thermal decomposition of diazomethane [37] whose activation energy is known to be nearly zero. On account of this value and a term of 0.4 eV [40] for the ¹A₁ state of CH₂ actual dissociation energy for the spin-forbidden process should be 1.2 eV. This is in good agreement with the value that we have obtained by simply plotting a parallel line (dashed line in “*T*” curve in Fig. 5) between our calculated curve and what should be the actual experimental one; this value is 1.4 eV.

- (3) The calculated value for BH₃CO should be retained as close to the actual value
- (4) The total energy value for BH₃N₂, calculated at a geometry close to that of BH₃CO was found to be less stable than the dissociation products so that the *D_e* value was put to 0. The instability of this molecule is then confirmed.

6. Conclusions

In this work, we have investigated the electronic structure of a set of isoelectronic molecules which dissociate to isoelectronic products.

The ground state equilibrium geometries derived with the 6-31G basis set are in good agreement with the corresponding experimental geometries, except for some specific parameters for which basis set deficiencies are discussed. The least energy dissociation path of the ground state of these molecules have been compared on the basis of electronic density interactions.

Finally quite reliable quantitative results have been obtained for the dissociation energies calculated with the 6-31G** polarized basis set and taking into account the correlation energy by use of a simple and economical method presented previously. These results confirm the applicability of this method for correlation energy calculations for non-trivial systems and permit us to precise some dissociation energy values: prediction of values for HNCO and BH₃CO where no experimental values exist, discussion of the experimental uncertainties for CH₂N₂ and confirmation of the instability of BH₃N₂.

Acknowledgments. The authors are grateful to the Belgian "Fonds de la Recherche Fondamentale Collective" (F.R.F.C.) for a research grant and to the "Ministère de la Politique Scientifique" for a "action de recherche concertée". They also thank Prof. G. Verhaegen for helpful discussions.

References

1. Lievin, J., Verhaegen, G.: *Theoret. Chim. Acta (Berl.)* **42**, 47 (1976), *Theoret. Chim. Acta (Berl.)* **45**, 269 (1977)
2. Lievin, J., Breulet, J., Verhaegen, G.: *Theoret. Chim. Acta (Berl.)* **52**, 75 (1979)
3. Lievin, J., Breulet, J., Verhaegen, G.: *Theoret. Chim. Acta (Berl.)* **60**, 339 (1981)
4. Binkley, J. S., Whitehead, R. A., Hariharan, P. C., Seeger, R.: GAUSSIAN 76, Program no 368, Q.C.P.E.
5. Davidson, E. R.: *Chem. Phys. Letters* **21**, 565 (1973)
6. Morokuma, K., Iwata, J.: Private communication
7. Hehre, W. J., Stewart, R. F., Pople, J. A.: *J. Chem. Phys.* **51**, 2657 (1969)
8. Hehre, W. J., Ditchfield, R., Pople, J. A.: *J. Chem. Phys.* **56**, 2257 (1972)
9. Hariharan, P. C., Pople, J. A.: *Theoret. Chim. Acta (Berl.)* **28**, 213 (1973)
10. Oksuz, I., Sinanoglu, O.: *Phys. Rev.* **181**, 42 (1969)
11. Whitten, J. L., Hackmeyer, M.: *J. Chem. Phys.* **51**, 5584 (1969)
12. Verhaegen, G., Moser, C. M.: *J. Phys. B: Atom. Molec. Phys.* **3**, 478 (1970)
13. Desclaux, J. P., Moser, C. M., Verhaegen, G.: *J. Phys. B: Atom. Molec. Phys.* **4**, 296 (1971)
14. Mulliken, R. S.: *J. Chem. Phys.* **33**, 1833 (1955)
15. Lichtenberger, L., Fenske, R. F.: MOPLOT, Program no 310, Q.C.P.E.
16. Williamson, H.: *C.A.C.M.* **15**, 100 (1972)
17. Shimanouchi, T.: in *Physical chemistry*, Vol. IV, Chapter 6. New York: Academic Press (1970)
18. Vucelic, M., Ohrn, Y., Sabin, J. R.: *J. Chem. Phys.* **59**, 3009 (1973)
19. Yamada, K.: *J. Molec. Spectrosc.* **79**, 323 (1980)
20. McLean, A. D., Loew, G. H., Berkowitz, D. S.: *J. Mol. Spectrosc.* **72**, 430 (1978)
21. Mallinson, P. D., Nemes, L.: *J. Mol. Spectrosc.* **59**, 470 (1976)
22. Dykstra, C. E.: *J. Chem. Phys.* **68**, 4244 (1978)
23. Pepin, C., Lambert, L., Cabana, A.: *J. Mol. Spectrosc.* **53**, 120 (1974)
24. Herzberg, G.: *Electronic spectra and electronic structure of polyatomic molecules*. New York: Van Nostrand Reinhold (1966)
25. Hopper, D. G., Wahl, A. C., Wu, R. L. C., Tiernan, T. O.: *J. Chem. Phys.* **65**, 5474 (1976)
26. Winnemisser, B. P.: *J. Mol. Spectrosc.* **82**, 220 (1980)
27. Harrison, S. W., Fisher, C. R., Kemmey, P. J.: *Chem. Phys. Letters* **36**, 229 (1975)
28. Moore, C. B., Pimentel, G. C.: *J. Chem. Phys.* **40**, 329 (1964)
29. Leroy G., Sana, M.: *Theoret. Chim. Acta (Berl.)* **33**, 329 (1974)
30. Whitten, J. L.: *J. Chem. Phys.* **39**, 349 (1963), *J. Chem. Phys.* **44**, 359 (1966)
31. JANAF Thermochemical Tables Nat. Bur. Standards (U.S.), **37** (1971)
32. Moore, C. E.: *Atomic Energy Levels*, Nat. Bur. Standards (U.S.), **35/V.I.**, 45 (1971)
33. Kajimoto, O., Yamamoto, T., Fueno, T.: *J. Phys. Chem.* **83**, 429 (1979)

34. Laufer, A. H., Okabe, H.: J.A.C.S. **93**, 4137 (1971)
35. Paulett, G. S., Ettinger, R.: J. Chem. Phys. **39**, 825 and 3524 (1963)
36. Frey, H. M., Stevens, I. D. R.: Proc. Chem. Soc. **79**, (1962)
37. Setser, D. W., Rabinovitch, B. S.: Canad. J. Chem. **40**, 1425 (1962)
38. Feldman, D., Meier, K., Zacharias, H., Welge, K. H.: Chem. Phys. Letters **59**, 171 (1978)
39. Simons, J. W., Curry, R.: Chem. Phys. Letters **38**, 171 (1976)
40. Harrison, J. F.: Accounts Chem. Res. **7**, 378 (1974)

Received October 8/November 9, 1981